

# Luminescent Triarylboron-Functionalized Zinc Carboxylate Metal–Organic Framework

Barry A. Blight,<sup>†</sup> Rémy Guillet-Nicolas,<sup>‡</sup> Freddy Kleitz,<sup>\*,‡</sup> Rui-Yao Wang,<sup>†</sup> and Suning Wang<sup>\*,†</sup>

<sup>†</sup>Department of Chemistry, Queen's University, Kingston, Ontario K7L 3N6, Canada

<sup>‡</sup>Department of Chemistry, Laval University, Quebec City, Quebec G1 V 0A6, Canada

## S Supporting Information

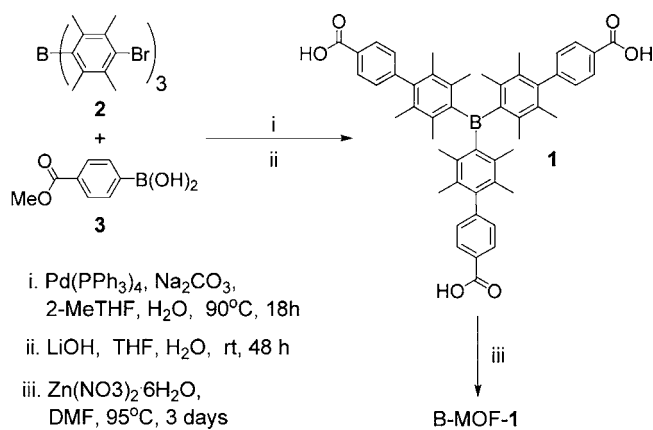
**ABSTRACT:** A luminescent triarylboron ligand functionalized with three carboxylic groups has been synthesized and fully characterized. Its use in boron-containing metal–organic frameworks (B-MOFs) has been demonstrated by the synthesis and isolation of a Zn<sup>II</sup>B-MOF compound (B-MOF-1). The crystals of B-MOF-1 belong to the cubic space group *F432* with 8-fold interpenetrated networks and ~21% void space. B-MOF-1 exhibits blue fluorescence and is capable of modest gas sorption of N<sub>2</sub>, argon, and CO<sub>2</sub>.

Carboxylate-based metal–organic frameworks (MOFs) are among the most extensively investigated and most robust MOF systems.<sup>1</sup> Recent research of MOFs has focused on the development of functional substrates that are capable of gas storage,<sup>2</sup> light harvesting,<sup>3</sup> catalysis,<sup>4</sup> proton conduction,<sup>5</sup> chemical sensing,<sup>6</sup> or drug delivery.<sup>7</sup> Examples of luminescent MOF systems are especially interesting because they may be used as highly effective sensory systems, where the origin of emission can be from either the backbone ligands,<sup>8</sup> the metal centers (e.g., many lanthanide-based MOFs),<sup>9</sup> or the luminescent guest molecules.<sup>10</sup> With the aim of developing potential solid-state sensing systems for gas molecules, we recently initiated the investigation of triarylboron-containing MOFs. This study is motivated by the fact that Lewis acidic triarylboron groups are usually luminescent and capable of binding to and sensing small guest molecules such as fluoride and cyanide.<sup>11</sup> Thus, the incorporation of triarylboron units into MOFs can provide new functionality and capability to the MOF architecture.

We have shown recently that the introduction of a carboxylate group to a triarylboron molecule can lead to facile syntheses of discrete triarylboron-containing bimetallic compounds such as copper(II) carboxylate paddlewheel complexes and lanthanide compounds.<sup>12</sup> We now report the extension of this system into three dimensions as the first example of a luminescent zinc(II) carboxylate metal–organoboron framework (B-MOF). The porosity and luminescent response of the new B-MOF toward gas uptake have been examined. The only previously reported examples of B-MOFs are based on a neutral linker tris(4-pyridyl)durylborane<sup>13</sup> and were not evaluated for gas-uptake capacities.

Ligand **1**, a C<sub>3</sub>-symmetric star-shaped molecule, was synthesized (Scheme 1) by Suzuki coupling of tris(4-bromoduryl)borane (**2**)<sup>14</sup> with excess boronic acid (**3**), yielding the triester (82% yield), followed by saponification with LiOH

**Scheme 1. Synthetic Procedures of L-1 and B-MOF-1**



(89% yield). Free ligand **1** exhibits purple-blue fluorescence at 397 nm ( $\lambda_{\text{ex}} = 330$  nm, THF, 298 K,  $\Phi = 0.03$ ), which is comparable to the monotopic carboxylate ligand that we previously reported.<sup>12</sup> Crystals<sup>15</sup> of **1** obtained from a toluene and methanol solution belong to the monoclinic space group *P2<sub>1</sub>/c*. In the crystal lattice, molecules of **1** form an extended, interweaved 2D hydrogen-bonded network via the three carboxylic groups, as shown in Figure 1. Toluene solvent molecules are found within and between the 2D networks of **1** (see the Supporting Information, SI).

The ability of ligand **1** to form B-MOFs is demonstrated by the successful synthesis of B-MOF-1 via solvothermal conditions by reacting ligand **1** and Zn(NO<sub>3</sub>)<sub>2</sub>·6H<sub>2</sub>O in *N,N*-dimethylformamide (DMF) at 95 °C for 3 days in a sealed tube. Single crystals of B-MOF-1, which nucleated on the side of the reaction vessel during the course of the reaction, were isolated in 62% yield. The crystalline solid exhibits blue emission characteristic of the triarylboron moiety at 402 nm ( $\lambda_{\text{ex}} = 330$  nm, 298 K,  $\Phi = 0.29$ ; see Figures S5 and S6 in the SI). Elemental analysis indicated that B-MOF-1 has the composition of Zn<sub>1.5</sub>[L-1<sup>3-</sup>](H<sub>2</sub>O)<sub>3</sub>[(NH<sub>2</sub>Me<sub>2</sub>)NO<sub>3</sub>](DMF)<sub>0.5</sub>, while X-ray diffraction (XRD) analysis confirmed that the B-MOF-1 framework has the composition of Zn<sub>1.5</sub>[L-1<sup>3-</sup>](H<sub>2</sub>O).

The crystal data<sup>15</sup> of B-MOF-1 were collected several times. The quality of the XRD data of B-MOF-1 is consistently poor because of the crystals' small dimensions and the difficulty in locating/modeling guest/salt molecules inside the lattice.

Received: September 17, 2012

Published: February 4, 2013



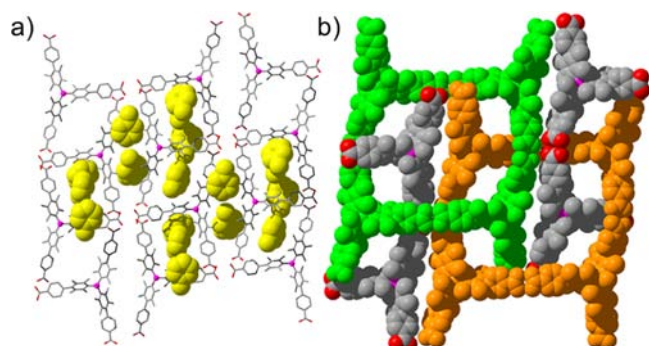


**Figure 1.** Crystal structure of ligand **1** (H atoms removed for clarity): (a) illustration of the hydrogen-bonded network and the locations of toluene molecules (pink, boron; gray, carbon; red, oxygen); (b) space-filling diagram showing the interweaving hydrogen-bonded network.

Nonetheless, we were able to establish the key features of the framework (Figures 2 and 3). B-MOF-1 belongs to the chiral

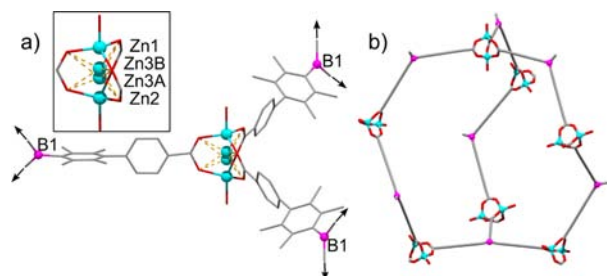


**Figure 2.** (a) Diagram showing the environment around the  $\text{Zn}^{\text{II}}$  ions and the disordered  $\text{Zn}^{\text{II}}$  sites (H atoms are omitted for clarity). (b) Diagram showing the single cage and connectivity in B-MOF-1. The central  $\text{Zn}^{\text{II}}$  ions (Zn3A and Zn3B) occupying the chelate sites and the aryl groups around the B atom are omitted (pink, boron; gray, carbon; red, oxygen; turquoise, zinc).

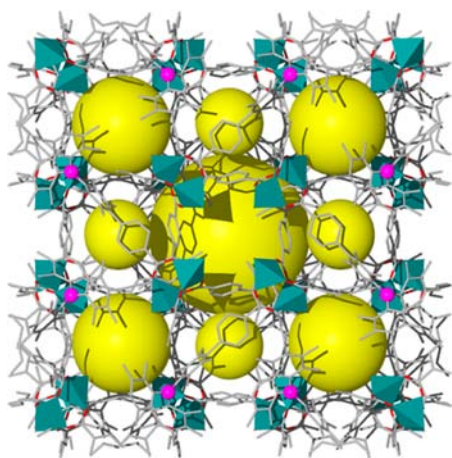


**Figure 3.** 3D structure of B-MOF-1 showing the porous spaces by yellow spheres (pink, boron; gray, carbon; red, oxygen; turquoise polyhedra, zinc).

cubic space group  $F432$ . There are two distinct environments for the  $\text{Zn}^{\text{II}}$  ions: dinuclear paddlewheel sites with tetrahedral geometry and mononuclear chelate sites with distorted octahedral geometry (Figure 2a). The  $\text{Zn}^{\text{II}}$  ions are disordered over these sites, with a total occupancy factor of  $\sim 80\%$  and  $\sim 20\%$  for the tetrahedral and octahedral sites, respectively (see the SI).

On the tetrahedral sites, the  $\text{Zn}^{\text{II}}$  ions are bound by four O atoms (three from the three bridging carboxylates and one from  $\text{H}_2\text{O}$ ). On the octahedral sites, the  $\text{Zn}^{\text{II}}$  ions are chelated by three carboxylates. Both B and Zn atoms occupy the  $C_3$  sites. The  $\text{Zn}^{\text{II}}$  ions and the trigonally arranged ligand **1** each serve as a triangular linker, forming a large chiral cage (Figure 2b) involving seven  $\text{Zn}^{\text{II}}$  units and seven boron units, which are further extended into a 3D 8-fold interpenetrated network via the same linkers (see Figure 2 and the SI). Compared to the crystals of ligand **1** that collapse rapidly upon removal from solution, the crystals of B-MOF-1 are highly robust and do not show any apparent change after being subjected to high vacuum, supporting the high stability of the B-MOF framework.

Despite the high degree of interpenetration, the crystals of B-MOF-1 possess modest porosity as revealed by X-ray data (21% of void space; pore volume of  $0.18 \text{ cm}^3 \text{ g}^{-1}$  calculated from the crystal density  $1.175 \text{ g cm}^{-3}$  accounting for  $\text{Zn}_{1.5}[\text{L}-1^{-3}](\text{H}_2\text{O})\cdot[(\text{NH}_2\text{Me}_2)\text{NO}_3]$ ). As shown in Figure 3, three different spherical void spaces of approximately 1.4, 0.7, and 0.2 nm in diameter are present in the crystal lattice. The porosity was further probed via gas physisorption analyses using both  $\text{N}_2$  and argon as the probe gases. The argon adsorption–desorption isotherms of B-MOF-1 are shown in Figure 4a as linear and semilogarithmic-scale plots.

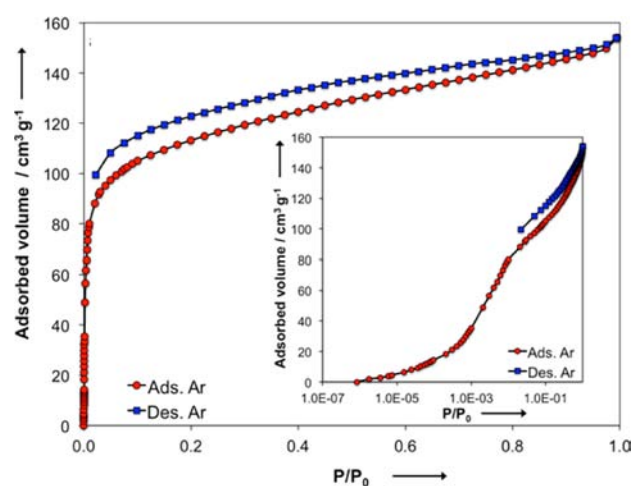


**Figure 4.** Adsorption–desorption isotherms of B-MOF-1 with Ar at 87 K. Inset: isotherms plotted in a semilogarithmic scale.

For comparison, the corresponding  $\text{N}_2$  adsorption data are presented in Figure S10 in the SI. In both cases, the isotherms are characteristic of a microporous material, with a type I isotherm, typical for most MOF materials.<sup>16</sup> The physicochemical parameters derived from the inert gas adsorption analysis are compiled in Table S2 in the SI. The argon Brunauer–Emmett–Teller specific surface area and pore volume obtained for B-MOF-1 are  $368 \text{ m}^2 \text{ g}^{-1}$  and  $0.19 \text{ cm}^3 \text{ g}^{-1}$ , respectively (ca.  $406 \text{ m}^2 \text{ g}^{-1}$  and  $0.21 \text{ cm}^3 \text{ g}^{-1}$  from the  $\text{N}_2$  sorption analysis), in good agreement with data from XRD analysis. Advanced pore-size analysis was performed by applying modern nonlocal density functional theory (NLDFT) method<sup>17</sup> on the argon data assuming a cylindrical pore model for zeolitic/oxidic pores (see the SI). The theoretical NLDFT isotherm fits the experimental data very well (see Figure S11 in the SI). The data indicate that B-MOF-1 consists of mainly micropores of diameters approximately 1.2 nm and less.

Both Ar and  $\text{N}_2$  isotherms show an adsorption–desorption hysteresis over a wide pressure range, with loops that never close;

i.e., low pressure adsorption hysteresis is observed as well. The cause of this phenomenon is not understood yet, and further investigation is required to properly characterize this effect. B-MOF-1 has also been found to adsorb CO<sub>2</sub> gas (see the SI).

In summary, we have successfully synthesized the first triarylboron-functionalized carboxylate MOF. Its structure exhibits an 8-fold interpenetrated network, leaving only small pores capable of modest gas uptake. Current efforts are focused on the synthesis of noninterpenetrated B-MOFs to create larger pore volumes and thus enhancement of the gas-uptake capacity.

## ■ ASSOCIATED CONTENT

### ■ Supporting Information

X-ray crystallographic data in CIF format, experimental data, syntheses, powder XRD pattern, photophysical properties, physisorption analysis, and X-ray crystal structure data. This material is available free of charge via the Internet at <http://pubs.acs.org>.

## ■ AUTHOR INFORMATION

### Corresponding Author

\*E-mail: [wangs@chem.queensu.ca](mailto:wangs@chem.queensu.ca) (S.W.), [freddy.kleitz@chm.ulaval.ca](mailto:freddy.kleitz@chm.ulaval.ca) (F.K.).

### Notes

The authors declare no competing financial interest.

## ■ ACKNOWLEDGMENTS

We thank the Natural Sciences and Engineering Council of Canada (NSERC) for financial support. B.A.B. thanks the NSERC for a Postdoctoral Fellowship. We are grateful to Matthias Thommes at Quantachrome Instruments for his efforts in CO<sub>2</sub> adsorption experiments.

## ■ REFERENCES

- (1) (a) Li, H.; Eddaoudi, M.; Groy, T. L.; Yaghi, O. M. *J. Am. Chem. Soc.* **1998**, *120*, 8571. (b) Li, H.; Eddaoudi, M.; O'Keeffe, M.; Yaghi, O. M. *Nature* **1999**, *402*, 276. (c) Kondo, M.; Yoshitomi, T.; Seki, K.; Matsuzaka, H.; Kitagawa, S. *Angew. Chem., Int. Ed. Engl.* **1997**, *36*, 1725. (d) Serre, C.; Férey, G. *Inorg. Chem.* **1999**, *38*, 5370. (e) Hirai, K.; Furukawa, S.; Kondo, M.; Uehara, H.; Hiromitsu, S.; Sakata, O.; Kitagawa, S. *Angew. Chem., Int. Ed.* **2011**, *50*, 8057. (f) O'Keeffe, M.; Yaghi, O. M. *Chem. Rev.* **2012**, *112*, 675. (g) Stock, N.; Biswas, S. *Chem. Rev.* **2012**, *112*, 933.
- (2) (a) Chen, B.; Eddaoudi, M.; Hyde, S. T.; O'Keeffe, M.; Yaghi, O. M. *Science* **2001**, *291*, 1021. (b) Rowsell, L. C.; Yaghi, O. M. *Angew. Chem., Int. Ed.* **2005**, *44*, 4670. (c) Spencer, E. C.; Howard, J. A. K.; McIntyre, G. J.; Rowsell, J. L. C.; Yaghi, O. M. *Chem. Commun.* **2006**, 278. (d) Doonan, C. J.; Tranchemontagne, D. J.; Glover, T. G.; Hunt, J. R.; Yaghi, O. M. *Nat. Chem.* **2010**, *2*, 235. (e) Han, D.; Jiang, F.-L.; Wu, M.-Y.; Chen, L.; Hong, M.-C. *Chem. Commun.* **2011**, 9861. (f) Suh, M. P.; Park, H. J.; Prasad, T. K.; Lim, D.-W. *Chem. Rev.* **2012**, *112*, 782. (g) Getman, R. B.; Bae, Y.-S.; Wilmur, R. C. E.; Snurr, Q. *Chem. Rev.* **2012**, *112*, 703.
- (3) (a) Lee, C. Y.; Farha, O. K.; Hong, B. J.; Sarjeant, A. A.; Nguyen, S. T.; Hupp, J. T. *J. Am. Chem. Soc.* **2011**, *133*, 15858. (b) Kent, C. A.; Liu, D.; Ma, L.; Papanikolas, J. M.; Meyer, T. J.; Lin, W. *J. Am. Chem. Soc.* **2011**, *133*, 12940.
- (4) (a) Seo, J. S.; Whang, D.; Lee, H.; Jun, S. I.; Oh, J.; Jeon, Y. J.; Kim, K. *Nature* **2000**, *404*, 982. (b) Xamena, F. X. L.; Abad, A.; Corma, A.; Garcia, H. *J. Catal.* **2007**, *250*, 294. (c) Lee, J. Y.; Farha, O. K.; Roberts, J.; Scheidt, K. A.; Nguyen, S. T.; Hupp, J. T. *Chem. Soc. Rev.* **2009**, *38*, 1450. (d) Ye, J.-Y.; Liu, C.-J. *Chem. Commun.* **2011**, 47, 2167. (e) Cohen, S. *Chem. Rev.* **2012**, *112*, 470. (f) Yoon, M.; Srirambalaji, R.; Kim, K. *Chem. Rev.* **2012**, *112*, 1196.

- (5) (a) Jeong, N. C.; Samanta, B.; Lee, C. Y.; Farha, O. K.; Hupp, J. T. *J. Am. Chem. Soc.* **2012**, *134*, 51. (b) Taylor, J. M.; Mah, R. K.; Ratcliffe, C. I.; Moudrakovski, I.; Vaidyanathan, R.; Shimizu, G. K. H. *J. Am. Chem. Soc.* **2010**, *132*, 14055. (c) Hurd, J. A.; Vaidyanathan, R.; Thangadurai, V.; Ratcliffe, C. I.; Moudrakovski, I. L.; Shimizu, G. K. H. *Nat. Chem.* **2009**, *1*, 705.

- (6) Kreno, L. E.; Leong, K.; Farha, O. K.; Allendorf, M.; Van Duyne, R. P.; Hupp, J. T. *Chem. Rev.* **2012**, *112*, 1105–1125.

- (7) (a) Zhao, H.; Jin, Z.; Su, H.; Jing, X.; Sun, F.; Zhu, G. *Chem. Commun.* **2011**, 47, 6389. (b) Horcajada, P.; Serre, C.; Maurin, G.; Ramsahye, N. A.; Balas, F.; Vallet-Regí, M.; Sebban, M.; Taulelle, F.; Férey, G. *J. Am. Chem. Soc.* **2008**, *130*, 6774. (c) Della Rocca, J.; Liu, D.; Lin, W. *Acc. Chem. Res.* **2011**, *44*, 957. (d) Horcajada, P.; Gref, R.; Baati, T.; Allen, P. K.; Maurin, G.; Couvreur, P.; Férey, G.; Morris, R. E.; Serre, C. *Chem. Rev.* **2012**, *112*, 1232.

- (8) (a) He, J.; Xu, Z.; Zeller, M.; Hunter, A. D. *J. Am. Chem. Soc.* **2012**, *134*, 1553. (b) Gole, B.; Bar, A. K.; Mukherjee, P. S. *Chem. Commun.* **2011**, 12137. (c) Wanderley, M. M.; Wang, C.; Wu, C.-D.; Lin, W. *J. Am. Chem. Soc.* **2012**, *134*, 9050. (d) Sapchenko, S. A.; Samsonenko, D. G.; Dybtsev, D. N.; Melgunov, M. S.; Fedin, V. P. *Dalton Trans.* **2011**, *40*, 2196.

- (9) (a) Zhan, C.-H.; Wang, F.; Kang, Y.; Zhang, J. *Inorg. Chem.* **2012**, *51*, 523. (b) Wang, H.-N.; Meng, X.; Qin, C.; Wang, X.-L.; Yang, G.-S.; Su, Z.-M. *Dalton Trans.* **2012**, *41*, 1047. (c) Ciu, Y.; Yue, Y.; Qian, G.; Chen, B. *Chem. Rev.* **2012**, *112*, 1126.

- (10) Wang, H.; Zhu, G. *Adv. Mater. Res.* **2012**, *345*, 245.

- (11) (a) Wade, C. R.; Broomsgrove, A. E. J.; Aldridge, S.; Gabbai, F. P. *Chem. Rev.* **2010**, *110*, 3958. (b) Hudnall, T. W.; Chiu, C. W.; Gabbai, F. P. *Acc. Chem. Res.* **2009**, *42*, 388. (c) Kubo, Y.; Yamamoto, M.; Ikeda, M.; Takeuchi, M.; Shinkai, S.; Yamaguchi, S.; Tamao, K. *Angew. Chem., Int. Ed.* **2003**, *42*, 2036. (d) Yamaguchi, S.; Akiyama, S.; Tamao, K. *J. Am. Chem. Soc.* **2001**, *123*, 11372. (e) Entwistle, C. D.; Marder, T. B. *Angew. Chem., Int. Ed.* **2002**, *41*, 2927. (f) Jäkle, F. *Chem. Rev.* **2010**, *110*, 3985. (g) Jäkle, F. *Coord. Chem. Rev.* **2006**, *250*, 1107. (h) Sun, Y.; Ross, N.; Zhao, S.-B.; Huszarik, K.; Jia, W.-L.; Wang, R.-Y.; Macartney, D.; Wang, S. *J. Am. Chem. Soc.* **2007**, *129*, 7510.

- (12) (a) Blight, B. A.; Stewart, A. F.; Wang, N.; Lu, J.-S.; Wang, S. *Inorg. Chem.* **2012**, *51*, 778. (b) Varlan, M.; Blight, B. A.; Wang, S. *Chem. Commun.* **2012**, DOI: 10.1039/C2CC36172H.

- (13) (a) Liu, Y.; Xu, X.; Xheng, F.; Cui, Y. *Angew. Chem., Int. Ed.* **2008**, *47*, 4538. (b) Liu, Y.; Xu, X.; Xia, Q.; Yuan, G.; He, Q.; Cui, Y. *Chem. Commun.* **2010**, 46, 2608.

- (14) Yamaguchi, S.; Shirasaka, T.; Tamao, K. *Org. Lett.* **2000**, *2*, 4129.

- (15) Crystal data of ligand **1** and B-MOF-1 have been deposited at the Cambridge Crystallographic Data Centre (CCDC 895409 and 895410).

- (16) (a) Senkovska, I.; Hoffmann, F.; Fröba, M.; Getzschmann, J.; Böhlmann, W.; Kaskel, S. *Microporous Mesoporous Mater.* **2009**, *122*, 93. (b) Schlichte, K.; Kratzke, T.; Kaskel, S. *Microporous Mesoporous Mater.* **2004**, *73*, 81. (c) Barthelet, K.; Marrot, J.; Riou, D.; Férey, G. *Angew. Chem., Int. Ed.* **2002**, *41*, 281.

- (17) (a) Thommes, M. *Chem. Ing. Tech.* **2010**, *82*, 1059. (b) Neimark, A. V.; Ravikovitch, P. I. *Microporous Mesoporous Mater.* **2001**, *44–45*, 697.